

Photochemical Substitution Reactions of Iron Tricarbonyl 1,4-Dimethyltetraazadiene and Related Complexes. Behavior Consistent with the Strong Coupling Limit

Curtis E. Johnson and William C. Trogler*

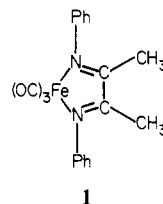
Contribution from the Department of Chemistry, Northwestern University, Evanston, Illinois 60202. Received March 23, 1981

Abstract: Photosubstitution of CO in $\text{Fe}(\text{CO})_3[\text{N}_4(\text{CH}_3)_2]$ and $\text{Fe}(\text{CO})_2[\text{P}(\text{C}_6\text{H}_5)_3][\text{N}_4(\text{CH}_3)_2]$ proceeds via a dissociative mechanism, in contrast to corresponding thermal reactions, which are of associative character. Syntheses of $\text{Fe}(\text{CO})_3[\text{N}_4(\text{CH}_3)_2]$, $\text{Fe}(\text{CO})_2\text{L}[\text{N}_4(\text{CH}_3)_2]$ [$\text{L} = \text{P}(\text{C}_6\text{H}_5)_3$, $\text{P}(\text{CH}_3)_3$, $\text{P}(\text{OCH}_3)_3$, and $\text{P}(\text{c-C}_6\text{H}_{11})_3$], $\text{Fe}(\text{CO})\text{L}_2[\text{N}_4(\text{CH}_3)_2]$ [$\text{L} = \text{P}(\text{C}_6\text{H}_5)_3$, $\text{P}(\text{CH}_3)_3$, and $\text{P}(\text{OCH}_3)_3$ and $\text{L}_2 = \text{dmpe}$] and $\text{Fe}[\text{P}(\text{OCH}_3)_3]_3[\text{N}_4(\text{CH}_3)_2]$ are reported. Quantum yields for CO substitution in the tricarbonyl complex increase exponentially as a function of excitation energy from 0.08 at 578 nm to 0.53 at 313 nm. The visible and near-ultraviolet absorptions in the electronic spectrum have been attributed to $\pi \rightarrow \pi^*$ transitions of the FeN_4 metalocycle. There is little correlation between the detailed wavelength dependence of the quantum yields and either the absorption spectrum or the nature of the lowest excited electronic states. Since the quantum yield-wavelength dependence suggests that photodissociation competes with vibrational relaxation, a weak coupling description is inappropriate. Ramifications of the strong coupling limit are explored, and we propose that the amount by which the irradiation energy exceeds the threshold for Fe-CO bond cleavage accounts for the observed wavelength dependence. Carbon monoxide photosubstitution in $\text{Fe}(\text{CO})_2[\text{P}(\text{C}_6\text{H}_5)_3][\text{N}_4(\text{CH}_3)_2]$ and $\text{Fe}(\text{CO})_3[\text{N}_2(\text{C}_6\text{H}_5)_2\text{C}_2(\text{CH}_3)_2]$ may also be explained in the strong coupling limit. Results for the latter complex further suggest a connection between the coordination environment about iron and the quantum efficiency of the photosubstitution process.

Photochemical reactions of transition-metal carbonyl complexes find frequent application in synthesis and catalysis.¹ It has been shown that ligand field excited states generally promote substitution reactions, whereas charge-transfer excited states are considerably less active²⁻⁷ in this regard. These rules have been applied with increasing generality, although efficient ligand dissociation may also be occurring from charge-transfer excited states in some instances.^{4,8-10} The photochemistry of highly covalent low-symmetry molecules, where the distinction between charge-transfer and ligand field excited states may not be possible, has not been studied in detail. Strong coupling models for excited-state reactivity might prove more appropriate in these systems, and iron tricarbonyl complexes present a test case for study.

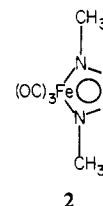
Interesting chemistry has developed on the basis of the tricarbonyliron moiety.¹¹ This functional group binds numerous olefinic substrates and can activate them toward nucleophilic attack.¹² Photosubstitution reactions of the iron-tricarbonyl fragment are of synthetic utility due to kinetic inertness of the $\text{Fe}(\text{CO})_3$ group. Pioneering studies by Von Gustorf and his group¹³ demonstrated efficient CO photosubstitution when $\text{Fe}(\text{CO})_3$ -(1,3-diene) complexes were excited with ultraviolet radiation. By

analogy to $\text{Fe}(\text{CO})_5$, "ligand field" excited states were assumed to mediate the substitution process. Metallacyclic $\text{Fe}(\text{CO})_3$ -(1,4-diazabutadiene) compounds such as **1** also lose the carbon



monoxide ligand upon UV photolysis.¹⁴ These complexes possess a low-energy (500-nm) electronic absorption band which has been attributed to a charge-transfer transition, and CO loss was reported to be inefficient upon irradiation into this band system.

We have recently studied¹⁵ the electronic structure of $\text{Fe}(\text{CO})_3(\text{N}_4\text{Me}_2)$ (**2**). A strong π interaction between the $\text{Fe}(\text{CO})_3$



(1) Geoffroy, G. L.; Wrighton, M. S. "Organometallic Photochemistry"; Academic Press: New York, 1979.

(2) Malouf, G.; Ford, P. C. *J. Am. Chem. Soc.* **1977**, *99*, 7213-7221.

(3) Wrighton, M. S.; Abrahamson, H. B.; Morse, D. L. *J. Am. Chem. Soc.* **1976**, *98*, 4105-4109.

(4) Giordano, P. J.; Wrighton, M. S. *Inorg. Chem.* **1977**, *16*, 160-166.

(5) Abrahamson, H. B.; Wrighton, M. S. *Inorg. Chem.* **1978**, *17*, 3385-3388.

(6) Dahlgren, R. M.; Zink, J. I. *Inorg. Chem.* **1977**, *16*, 3154-3161. In-corriva, M. J.; Zink, J. *Ibid.* **1978**, *17*, 2250-2253.

(7) Figard, J. E.; Peterson, J. D. *Inorg. Chem.* **1978**, *17*, 1059-1063.

(8) Mann, K. R.; Gray, H. B. *J. Am. Chem. Soc.* **1977**, *99*, 306-307.

(9) Balk, R. W.; Snoeck, T.; Stufkens, D. J.; Oskam, A. *Inorg. Chem.* **1980**, *19*, 3015-3021.

(10) Garratt, A. P.; Thompson, H. W. *J. Chem. Soc.* **1934**, 1817-1822.

(11) Collman, J. P.; Hegedus, L. S. "Principles and Applications of Organotransition Metal Chemistry"; University Science Books: Mill Valley, Calif. 1980; pp 617-632.

(12) Pettit, R.; Emerson, G. F. *Adv. Organomet. Chem.* **1964**, *1*, 1-46; "The Organic Chemistry of Iron"; Von Gustorf, E. A. K.; Grevels, F.-W., Fischer, I., Eds.; Academic Press: New York, 1978; Vol. 1.

(13) Von Gustorf, E. A. K.; Leenders, L. H. G.; Fischer, I.; Perutz, R. N. *Adv. Inorg. Chem. Radiochem.* **1976**, *19*, 65-183. Bock, C. R.; Von Gustorf, E. A. K. *Adv. Photochem.* **1977**, *10*, 222-310. Jaenicke, O.; Kerber, R. C.; Kirsch, P.; Von Gustorf, E. A. K.; Rumin, R. *J. Organomet. Chem.* **1980**, *187*, 361-373.

group and a π^* orbital of the tetraazadiene ligand yields a low-lying unoccupied metalocycle π^* orbital. One-electron transitions to this level occur in the visible and near-UV spectral regions. Considering the nature of these excited states and the analogy with diazabutadiene complexes, it was quite surprising to observe efficient CO photodissociation upon visible irradiation of **2**. In order to better understand the factors that influence photodissociative processes in these systems, we have examined the photochemistry of **1**, **2**, and $\text{Fe}(\text{CO})_2[\text{P}(\text{C}_6\text{H}_5)_3](\text{N}_4\text{Me}_2)$ in detail.

Experimental Section

Abbreviations Used. Me = methyl, Et = ethyl, Ph = phenyl, c-Hx = cyclohexyl, *t*-Bu = *tert*-butyl, *o*-tol = *o*-tolyl, *p*-tol = *p*-tolyl, THF =

(14) Fruhauf, H. W.; Grevels, F. W.; Landers, A. *J. Organomet. Chem.* **1979**, *178*, 349-360.

(15) Trogler, W. C.; Johnson, C. E.; Ellis, D. E. *Inorg. Chem.* **1981**, *20*, 980-986.

tetrahydrofuran, diphos = bis(1,2-diphenylphosphino)ethane, dmpe = bis(1,2-dimethylphosphino)ethane, L = two-electron donor ligand, R = alkyl, aryl, alkoxy, or aryloxy substituent, DAB = 1,4-diazabutadiene, and Φ = quantum yield for CO substitution.

Materials and General Procedures. Most compounds were purchased and used as received. Iron pentacarbonyl (Strem) was vacuum distilled, $\text{P}(\text{OMe})_3$ (Aldrich) was vacuum distilled from sodium, pyridine (Aldrich) was distilled from KOH, $\text{P}(p\text{-tol})\text{PH}_2$ (ROC/RIC) was recrystallized from ethanol, butadiene (Matheson, CP) was purified by trap-trap distillation, ferrocene was recrystallized from cyclohexane and sublimed, and PPh_3 (Aldrich) was recrystallized from ethanol. Methylazide¹⁶ and $\text{Fe}_2(\text{CO})_9$ ¹⁷ were prepared by literature methods. *Caution! Methylazide is an explosive.* Solvents were distilled under nitrogen from appropriate drying agents (sodium benzophenone, LiAlH_4 , P_2O_{10} , or CaH_2). The ligand $\text{P}(c\text{-Hx})_3$ was generously provided by Mr. Ralph Paonessa. All of the iron carbonyl compounds are air-sensitive and were handled by conventional high vacuum line and inert atmosphere techniques.¹⁸

Thermal Reactions. Preparation of $\text{Fe}(\text{CO})_3(\text{N}_4\text{Me}_2)$ (2). To a Schlenk flask equipped with a dry ice condenser was added 9.5 g (26 mmol) of $\text{Fe}_2(\text{CO})_9$ and 60 mL of Et_2O . After the mixture was cooled to 0 °C, 4.5 mL (69 mmol) of MeN_3 was added. The solution was stirred (allowing to warm to room temperature) for 48 h in the dark. The solution was filtered to remove suspended impurities and evaporated to dryness in vacuo (thereby removing $\text{Fe}(\text{CO})_5$ side product, identified by IR). The solid residue was redissolved in the minimum amount of CH_2Cl_2 , the solution chromatographed on silica gel (2.5 × 52 cm column), eluted with CH_2Cl_2 , and the second major band (deep red) was collected. The first band (orange) contains the previously reported¹⁹ ureylene complex $\text{Fe}_2(\text{CO})_6(\text{N}(\text{Me})\text{C}(\text{O})\text{N}(\text{Me}))$ (IR (hexanes) 2086 (m), 2048 (s), 2006 (s), 1991 (m), 1752 (m), 627 (w), 567 (m) cm^{-1} ; ^1H NMR (benzene) δ 2.18; mass spectrum (10 eV), parent ion at m/e 366). The solvent was removed from the second fraction under vacuum and the mixture sublimed (room temperature, 10^{-3} torr) to give 0.60 g (5% based on Fe) of the slightly air-sensitive tetraazadiene complex 2: IR (hexanes) 2068 (m), 1995 (s), 1959 (w) (^{13}C O), 1280 (w), 1203 (w), 996 (w), 814 (w), 637 (w), 620 (w), 565 (w) cm^{-1} ; UV-visible maximum (benzene) 467 nm (ϵ 2650), 342 (3890); ^1H NMR (C_6D_6) δ 3.89; $^{13}\text{C}\{^1\text{H}\}$ NMR (THF- d_6 with ~15 mg of $\text{Cr}(\text{acac})_3$ added) δ 211.3 (CO); ^{14}N NMR (CDCl_3) δ -54 (line width 240 Hz); mass spectrum (15 eV), parent ion at m/e 226. A single-crystal X-ray diffraction study of one of our samples by Professor R. Doedens of the University of California, Irvine,²⁰ conclusively establishes the molecular structure.

Preparation of $\text{Fe}(\text{CO})_3[\text{N}_4(\text{CD}_3)_2]$. We used $(\text{CD}_3)_2\text{SO}_4$ (International Chemical and Nuclear Corp., 99% D) to prepare N_3CD_3 and continued as in the preceding synthesis. Mass spectrometric analysis (10 eV) revealed the parent ion at m/e 232 and no non D_6 material was evident.

$\text{Fe}(\text{CO})_3[\text{PhNC}(\text{Me})\text{C}(\text{Me})\text{NPh}]$ (1), was prepared by the literature method²¹ and characterized by IR, NMR, UV-visible, and mass spectra.

Reaction between 2 and Trivalent Phosphorus Ligands. Typical reactions between 0.01 M 2 and 0.02 M ligand in toluene or benzene yielded $\text{Fe}(\text{CO})_2\text{L}(\text{N}_4\text{Me}_2)$ (L = PPh_3 , PMe_3 , $\text{P}(\text{OMe})_3$, $\text{P}(c\text{-Hx})_3$, $\text{P}(\text{OPh})_3$, PMePh_2) with respective reaction half-lives, in minutes (at T in °C) of [200 (110), <1 (25), 400 (25), 60 (110), 2000 (110), 300 (25)]. Isolation procedures below follow removal of solvent in vacuo. $\text{Fe}(\text{CO})_2(\text{PPh}_3)(\text{N}_4\text{Me}_2)$ was recrystallized from hot hexanes: IR (cyclohexane) 1988 (s), 1935 (s) cm^{-1} ; UV-visible max (benzene) 500 nm (ϵ 2100), 392 (4250), 368 (sh, 3640); ^1H NMR (C_6D_6) δ 3.79 (d, J = 2.1 Hz, NCH_3), 6.93–7.21 (m, C_6H_5); $^{31}\text{P}\{^1\text{H}\}$ NMR (4:1 THF/ C_6H_6) δ 62.7; mass spectrum (10 eV), parent ion at m/e 460. Anal. Calcd for $\text{FeC}_{22}\text{H}_{21}\text{N}_4\text{O}_2\text{P}$: C, 57.41; H, 4.60; N, 12.17. Found: 57.30; H, 4.66; N, 11.78. $\text{Fe}(\text{CO})_2(\text{PMe}_3)(\text{N}_4\text{Me}_2)$ was recrystallized from hexanes: IR (cyclohexane) 1989 (s), 1933 (s), cm^{-1} ; UV-visible maximum (benzene) 495 nm (ϵ 2550), 369 (3710); ^1H NMR (C_6D_6) δ 4.22 (s, 6 H, NCH_3), 0.47 (d, 9 H, J = 10.1 Hz, PCH_3); $^{31}\text{P}\{^1\text{H}\}$ NMR (toluene- d_6) δ 24.2; mass spectrum (10 eV), parent ion at m/e 274. $\text{Fe}(\text{CO})_2[\text{P}(\text{OMe})_3](\text{N}_4\text{Me}_2)$ was recrystallized from hexanes: IR (cyclohexane) 2009 (s), 1952 (s) cm^{-1} ; UV-visible max (benzene) 471 nm (ϵ 3060), 349 (3920); ^1H NMR (C_6D_6) δ 4.26 (d, 6 H, J = 4.8 Hz, NCH_3), 2.78 (d, 9 H, J = 12.1 Hz, POCH_3); $^{31}\text{P}\{^1\text{H}\}$ NMR (C_6D_6) δ 176.4. $\text{Fe}(\text{CO})_2$ -

$(\text{PCy}_3)(\text{N}_4\text{Me}_2)$ was recrystallized from hot hexanes: IR (cyclohexane) 1980 (s), 1924 (s) cm^{-1} ; ^1H NMR (C_6D_6) δ 4.33 (d, 6 H, J = 1.0 Hz, NCH_3), 1.58 and 1.00 (br, 33 H, C_6H_{11}); $^{31}\text{P}\{^1\text{H}\}$ NMR (4:1 THF/ C_6D_6) δ 70.3. $\text{Fe}(\text{CO})_2[\text{P}(\text{OPh})_3](\text{N}_4\text{Me}_2)$ was not isolated: IR (toluene) 2015 (s), 1958 (s) cm^{-1} ; ^1H NMR (toluene- d_6) δ 3.93 (d, J = 5.8 Hz, NCH_3), 6.93 (OC_6H_5). $\text{Fe}(\text{CO})_2(\text{PMePh}_2)(\text{N}_4\text{Me}_2)$ was not isolated: IR (heptane) 1988 (s), 1934 (s) cm^{-1} ; ^1H NMR (C_6D_6) δ 3.86 (d, 6 H, J = 1.6 Hz, NCH_3), 1.25 (d, 3 H, J = 8.9 Hz, PCH_3).

Photochemical Reactions. Photochemical Syntheses of $\text{Fe}(\text{CO})(\text{L})_2(\text{N}_4\text{Me}_2)$ Complexes. These reactions were generally performed in hexane solvent at room temperature. Usually an excess of L was employed except when L = $\text{P}(\text{OCH}_3)_3$, exactly 2 equiv were required to avoid formation of the trisubstituted complex. In a typical reaction 0.077 g (0.34 mmol) of 2 was dissolved in 30 mL of hexanes in a 50-mL Schlenk flask. After adding 150 μL (1.8 mmol) of PMe_3 , the solution was photolyzed for 46 h with a 450-W Xenon arc lamp (using a Corning 3-73 filter). The solution became colorless and a green precipitate of $\text{Fe}(\text{CO})(\text{PMe}_3)_2(\text{N}_4\text{Me}_2)$ formed. It was collected by filtration and recrystallized from toluene-hexane: IR (benzene) 1894 (s) cm^{-1} ; ^1H NMR (C_6D_6) δ 4.39 (3 H, NCH_3), 4.09 (3 H, NCH_3), 0.75 (m, second order, outside peaks at δ 0.80, 0.70 (8.4 Hz), 18 H, PCH_3); $^{31}\text{P}\{^1\text{H}\}$ NMR (C_6D_6) δ 22.0; mass spectrum (10 eV), parent ion at m/e 322.

Other $\text{Fe}(\text{CO})\text{L}_2(\text{N}_4\text{Me}_2)$ compounds prepared by the photochemical method are the following: $\text{Fe}(\text{CO})(\text{PPh}_3)_2(\text{N}_4\text{Me}_2)$, which was recrystallized from toluene-hexanes: IR (benzene) 1908 (s) cm^{-1} ; ^1H NMR (C_6D_6) δ 6.94 (m, 30 H, C_6H_5), 4.05 (3 H, NCH_3), 3.11 (3 H, NCH_3); $^{31}\text{P}\{^1\text{H}\}$ NMR (4:1 THF/ C_6D_6) δ 68.5; the compound was not sufficiently volatile to obtain a mass spectrum. Anal. Calcd for $\text{FeC}_{39}\text{H}_{36}\text{N}_4\text{O}_2\text{P}_2$: C, 67.45; H, 5.22; N, 8.07. Found: C, 66.71; H, 5.38; N, 7.96. $\text{Fe}(\text{CO})[\text{P}(\text{OMe})_3]_2(\text{N}_4\text{Me}_2)$ was prepared by photolyzing a solution of 2 and only 2 equiv of $\text{P}(\text{OMe})_3$. The bis(phosphite) compound was purified by recrystallization from hexanes (in which the tris(phosphite) compound is essentially insoluble and the mono(phosphite) compound is relatively soluble): IR (toluene) 1935 (s) cm^{-1} ; ^1H NMR (C_6D_6) δ 4.48 (t, 6 H, J = 2.5 Hz, NCH_3), 3.07 (second order, 18 H, POCH_3); $^{31}\text{P}\{^1\text{H}\}$ NMR (C_6D_6) δ 185.1. $\text{Fe}(\text{CO})[\text{P}(c\text{-Hx})_3]_2(\text{N}_4\text{Me}_2)$ was not isolated: IR (cyclohexane) 1893 (s) cm^{-1} ; ^1H NMR (C_6D_6) δ 4.22 (3 H, NCH_3), 3.15 (3 H, NCH_3); $^{31}\text{P}\{^1\text{H}\}$ NMR (4:1 THF/ C_6D_6) δ 74.8. Photolysis of 2 and excess $\text{P}(\text{OPh})_3$ only gave the mono(phosphite) complex and perhaps a little of $\text{Fe}(\text{CO})[\text{P}(\text{OPh})_3]_2(\text{N}_4\text{Me}_2)$: IR (toluene) ~1930 (sh, vw) cm^{-1} ; ^1H NMR (C_6D_6) δ 3.89 (d, 6 H, J = 5.8 Hz, NCH_3), 2.08 (9 H, tolyl CH_3); $^{31}\text{P}\{^1\text{H}\}$ NMR (4:1 THF/ C_6D_6) δ 165.0. $\text{Fe}(\text{CO})[\text{P}(o\text{-tolyl})_3]_2(\text{N}_4\text{Me}_2)$ was not isolated: $^{31}\text{P}\{^1\text{H}\}$ NMR (4:1 THF/ C_6D_6) δ 168.2. $\text{Fe}(\text{CO})_2(\text{py})(\text{N}_4\text{Me}_2)$ was not isolated: IR (benzene) 1989 (s), 1920 (s) cm^{-1} ; ^1H NMR (C_6D_6) δ 3.76 (NCH_3).

Photochemical Synthesis of $\text{Fe}[\text{P}(\text{OMe})_3]_3(\text{N}_4\text{Me}_2)$. The preparation followed the procedure used to prepare the disubstituted compounds except an excess of $\text{P}(\text{OMe})_3$ was employed and irradiation continued until the trisubstituted product precipitated. Violet $\text{Fe}[\text{P}(\text{OMe})_3]_3(\text{N}_4\text{Me}_2)$ was recrystallized from toluene-hexanes: IR (benzene) showed no peaks in the terminal CO region; ^1H NMR (CDCl_3) δ 4.08 (br, 6 H, NCH_3), 3.33 (m, second order, 27 H, POCH_3), in C_6D_6 the N -methyl peak resolved into a quartet (J = 1.2 Hz) at δ 4.43; $^{31}\text{P}\{^1\text{H}\}$ NMR (C_6D_6) δ 189.2; mass spectrum (15 eV), parent ion at m/e 514. Anal. Calcd for $\text{FeC}_{11}\text{H}_{33}\text{N}_4\text{O}_9\text{P}_3$: C, 25.70; H, 6.42; N, 10.90; P, 18.07. Found: C, 25.80; H, 6.52; N, 10.77; P, 18.14.

Quantum Yield Determinations. The radiation source was either a 200-W mercury-xenon lamp (Oriol 8500 power supply) or an Osram super pressure HBO 500-W mercury arc lamp in an Oriol housing (f /1.0 quartz lens and 10-cm water filter). Both power supplied maintained the light output to within $\pm 1\%$ (for a $\pm 10\%$ change in line voltage). The light was monochromatized with a Beckman 2400 DU spectrophotometer (half-intensity bandwidth of 5 nm at 313 and 334 nm and 10 nm at 366, 404, 436, 468, 546, and 578 nm). When an Edmund 436-nm interference filter was added, the quantum yields at 436 nm were unchanged (actinometry redone), verifying that there is not appreciable leakage of UV light through the monochromator. The cell compartment was thermostated to maintain the temperature within ± 0.5 °C of 25 °C, unless otherwise specified. Light intensities were determined by ferrioxalate,^{22,23} Reinecke's salt,²⁴ or Aberchrome²⁵ 540 (from Aberchromics Ltd., Aberystwyth, Dyfed, Wales, U.K.) actinometry. The reusable Aberchrome actinometer was calibrated with ferrioxalate actinometry.²⁶

(16) Dimroth, O.; Wislicenus, W. *Chem. Ber.* **1905**, *38*, 1573–1576.

(17) Braye, E. H.; Hubel, W. *Inorg. Synth.* **1966**, *8*, 178–181.

(18) Shriver, D. F. "The Manipulation of Air-Sensitive Compounds"; McGraw-Hill: New York, 1969.

(19) Dekker, M.; Knox, G. R. *J. Chem. Soc., Chem. Commun.* **1967**, 1243–1244.

(20) Private communication. The first structural study of a tetraazadiene complex may be found in Doedens, R. J. *J. Chem. Soc., Chem. Commun.* **1968**, 1271–1272.

(21) Otsuka, S.; Yoshida, T.; Nakamura, A. *Inorg. Chem.* **1967**, *6*, 20–25.

(22) Hatchard, C. G.; Parker, C. A. *Proc. R. Soc. London, Ser. A* **1956**, *235*, 518–536; Calvert, J. G.; Pitts, J. N. "Photochemistry"; Wiley: New York, 1966; pp 783–786.

(23) Bowman, W. D.; Demas, J. N. *J. Phys. Chem.* **1976**, *80*, 2434–2435.

(24) Wegner, E. E.; Adamson, A. W. *J. Am. Chem. Soc.* **1966**, *88*, 394–404.

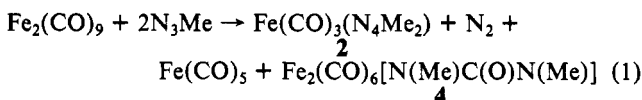
(25) Heller, H. G. *Chem. Ind. (London)* **1978**, 193–196.

Monochromatic light intensities were between 1×10^{-8} and 5×10^{-7} einsteins/min.

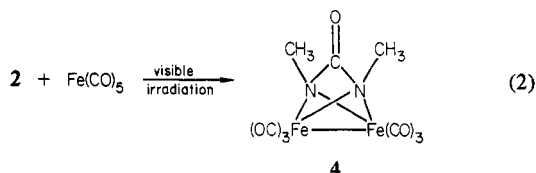
Extinction coefficients of reactants and products were determined from isolated and recrystallized compounds (with the exception of $\text{Fe}(\text{CO})_2(\text{PPh}_3)(\text{DAB})$, for which the ϵ data was taken from the final spectrum) and are given in Table SI of the supplementary material. Quantum yield reactions were monitored spectrophotometrically at low (2–15%) conversions, and the inner-filter and secondary photolysis corrections were always less than 5%. In a few cases the quantum yields exhibited a small dependence on the percent conversion and the initial value was calculated from extrapolation of a ϕ vs t plot. We estimate $\pm 15\%$ accuracy in the absolute quantum yields, although the reproducibility was somewhat better.

Results and Discussion

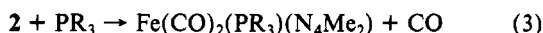
Thermal Reactions. The synthesis of **2** followed the procedure communicated¹⁹ by Dekker and Knox.



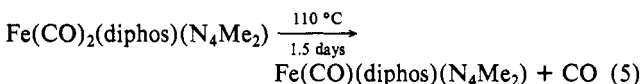
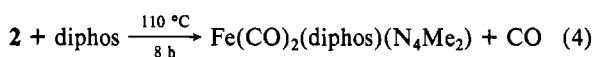
Yields of **2** varied from 5 to 15% and $\text{Fe}(\text{CO})_5$ and the dimeric ureylene **4** formed in yields comparable to **2**. About 30–40% of pyrophoric iron metal was produced as a byproduct. It is best to perform the synthesis and isolation in the dark to avoid the photochemical reaction (see supplementary material for details).



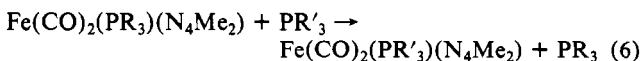
Although free tetraazadiene ligands are unknown, the iron complex is quite robust. No decomposition of **2** occurred, even after 70 h of refluxing in toluene. In the presence of trivalent phosphorus ligands, CO substitution may occur.



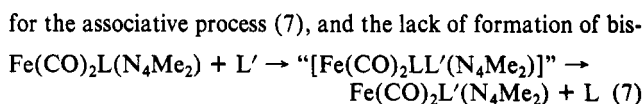
Bis(phosphine) compounds are not easily formed in reaction 3. During 30 h of refluxing in toluene, neither PMe_3 nor $\text{P}(\text{OMe})_3$ yielded a bis(phosphine) complex; however, in the presence of the chelating ligand bis(1,2-diphenylphosphino)ethane (diphos) one observes substitution of a second CO ligand (see supplementary material for details).



Mechanistic Aspects. Detailed kinetic studies²⁷ of reaction 3 establish an associative mechanism for the first CO substitution process. According to the above reactivity patterns one might also conclude that monodentate ligands cannot associatively attack the mono(phosphine) complexes; however, the substitution reaction (6) does take place. Again, an associative mechanism appears



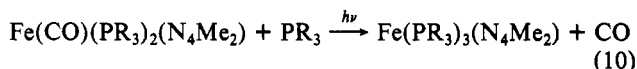
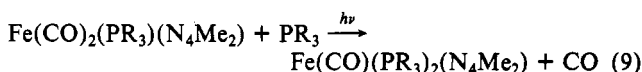
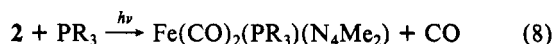
likely from the following experiments. While $\text{Fe}(\text{CO})_2(\text{PPh}_3)(\text{N}_4\text{Me}_2)$ rapidly substitutes at room temperature (when $\text{R}' = \text{Me}$), the analogous reaction with $\text{R}' = \text{c-Hx}$ does not occur during 13 h of refluxing in toluene. Furthermore, $\text{Fe}(\text{CO})_2[\text{P}(\text{c-Hx})_3](\text{N}_4\text{Me}_2)$ does not undergo reaction with PPh_3 during 13 h at 110°C , ruling out the possibility of an unfavorable equilibrium. Large phosphines do not substitute rapidly, as expected



(phosphine) products requires exclusive loss of L or L' from the six-coordinate intermediate in eq 7. The remaining question pertains to the reaction between **2** and diphos (reaction 5). A chelate *must* be bound cis in the presumed pseudooctahedral transition state of eq 7 while the monodentate phosphorus ligands L and L' are probably trans. Strong donor ligands would be expected to enhance Fe–CO back-bonding as well as to promote trans loss of L from the electron-rich transition state (for monodentate ligands).

Photochemical Reactions. As detailed in the supplementary material, visible light photolysis of **2** (in hexanes, cyclohexane, benzene, CH_2Cl_2 , THF, or CH_3CN) results in loss of CO to yield an unstable species, **3**, which appears to be a dimer of approximate composition $[\text{Fe}(\text{CO})_2(\text{N}_4\text{Me}_2)]_2$.

In the presence of trivalent phosphorus ligands, photolysis of **2** leads to clean ligand substitution as in reaction 8 and no **3** forms.



Secondary photolysis may also occur as in reactions 9 and 10. Initial IR and ^{31}P NMR spectra of these photolyzed solutions only contain an additional peak attributable to the monosubstituted product and establish that the disubstituted complexes form by reaction 9. Only the small π -acid ligand $\text{P}(\text{OMe})_3$ underwent process 10. Stepwise loss of CO cannot be taken for granted since recent vapor-phase photochemical studies²⁸ of $\text{Fe}(\text{CO})_5$ show that two CO's may be expelled (with $\Phi = 0.35$) in a primary photochemical process. All reactants and products appear to be distorted square pyramidal, with the N_4Me_2 chelate in the basal plane.²⁹

Mechanistic Aspects. In contrast to thermal reactions described earlier, the photochemical substitution processes proceed by a dissociative pathway.

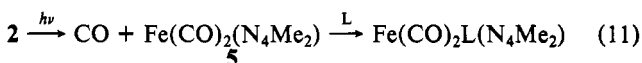


Table I collects quantum yield (Φ) data for reaction 11 with $\text{L} = \text{PPh}_3$. To prevent formation of **3**, at least a twofold excess of L must be present. There appears to be no statistically significant dependence of Φ 's upon the $[\text{PPh}_3]$ and addition of CO decreases Φ . A process involving partial dissociation of the tetraazadiene ligand (which is unstable as a free species) seems unlikely since ligand concentrations as high as 2 M have no significant effect on the reaction. In cases such as $\text{Fe}(\text{CO})_3(\text{diene})$, partial photochemical decomplexation to $(\eta^2\text{-diene})$ iron intermediates can ultimately lead to diene replacement.^{13,30} If the reaction proceeds

(28) Nathanson, G.; Gitlin, B.; Rosan, A. M.; Yardley, J. T. *J. chem. Phys.* **1981**, *74*, 361–369.

(29) Johnson, C. E.; Trogler, W. C. *Inorg. Chem.*, in press.

(30) Ellerhorst, G.; Gerhartz, W.; Grevels, F.-W. *Inorg. Chem.* **1980**, *19*, 67–71.

(31) Robinson, G. W.; Frosch, R. P. *J. Chem. Phys.* **1962**, *37*, 1962–1973; **1963**, *38*, 1187–1203.

(32) Ford, P. C. *Inorg. Chem.* **1975**, *14*, 1440–1441. Bergkamp, M. A.; Brannon, J.; Magde, D.; Watts, R. J.; Ford, P. C. *J. Am. Chem. Soc.* **1979**, *101*, 4549–4554. Thomas, T. R.; Watts, R. J.; Crosby, G. A. *J. Chem. Phys.* **1973**, *59*, 2123–2131. Petersen, J. D.; Watts, R. J.; Ford, P. C. *J. Am. Chem. Soc.* **1976**, *98*, 3188–3194. Petersen, J. D.; Ford, P. C. *J. Phys. Chem.* **1974**, *78*, 1144–1149. Watts, R. J.; Efrima, S.; Metiu, H. *J. Am. Chem. Soc.* **1979**, *101*, 2742–2743.

(33) Chock, D. P.; Jortner, J.; Rice, S. A. *J. Chem. Phys.* **1968**, *49*, 610–626. Freed, K. F.; Jortner, J. *Ibid.* **1969**, *50*, 2916–2927. Bixon, M.; Jortner, J. *Ibid.* 4061–4070. Band, Y. B.; Freed, K. F. *Ibid.* **1976**, *63*, 3382–3397.

(26) Heller, H. G.; Langan, J. R. *J. Chem. Soc., Perkin Trans. 2* **1981**, 341–343.

(27) Chang, C. Y.; Johnson, C. E.; Richmond, T. G.; Chen, Y. T.; Trogler, W. C.; Basolo, F. *Inorg. Chem.*, in press.

Table I. Quantum Yields for CO Photosubstitution by PPh_3 in 2^a

λ_{irr} , nm	$10^3 C_{\text{Fe}}$, M	$10^3 C_{\text{PPh}_3}$, M	Φ	Φ_{av}^b
578	32.2	327	0.08	0.08
578	32.2	327	0.08	
546	9.90	104	0.08	
546	9.84	116	0.08	0.07
546	5.35	110	0.07	
468	0.63	3.28	0.13 ^c	0.13
436	8.69	86.9	0.25	
436	5.35	110	0.19	
436	3.90	1950	0.25	
436	3.90	380	0.23	
436	3.90	21	0.22	0.21
436	1.11	125	0.18	
436	1.05	5.60	0.18	
436	0.55	3.44	0.19	
436	0.55	3.44	0.13 ^d	
404	3.87	28.5	0.22 ^e	0.22
366	27.7	335	0.22	
366	8.69	86.9	0.24	0.23
366	3.24	42.8	0.24	
366	0.64	3.37	0.24	
334	0.63	3.27	0.36 ^c	0.36
313	8.69	86.9	0.44	
313	0.65	3.37	0.50	
313	0.17	0.89	0.52	0.53
313	0.17	0.87	0.66	
313	0.14	0.75	0.52	

^a All photoreactions at 25 °C in benzene solutions. ^b Mean value for a specific irradiation wavelength; absolute error of quantum yields estimated to be $\pm 15\%$. ^c The same solution gave $\Phi = 0.24$ at 366 nm. ^d Added 730 torr of CO above solution, giving a solution CO concentration of 6.6×10^{-3} M. ^e As a check, continued irradiation of the sample gave $\Phi = 0.25$ at 366 nm.

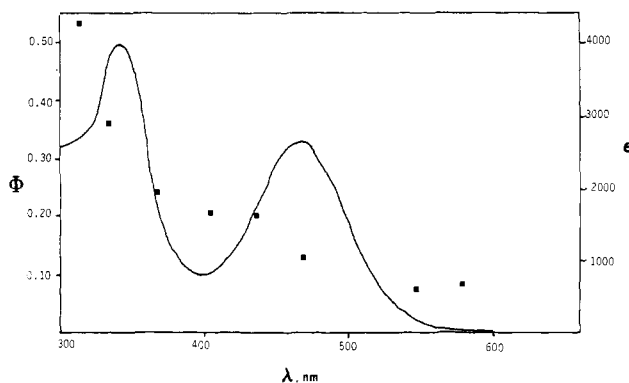
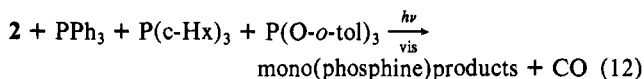


Figure 1. Quantum yields for the photosubstitution reaction $2 + \text{PPh}_3 \rightarrow \text{Fe}(\text{CO})_2(\text{PPh}_3)(\text{N}_4\text{Me}_2) + \text{CO}$ are plotted vs. wavelength and a spectrum of **2** is included for comparative purposes.

via **5**, we would expect it to be extremely reactive and show little preference for entering nucleophiles. The following reaction was monitored by ^{31}P NMR spectroscopy.



Integration of phosphorus NMR peaks (before significant secondary photolysis occurred) gave the relative yield of mono-phosphine products from PPh_3 , $\text{P}(\text{c-Hx})_3$, and $\text{P}(\text{O-}o\text{-tol})_3$ of 3:3:1. The small degree of discrimination contrasts with that observed²⁷ for the associative thermal reactions.

Nature of the Lowest Excited States. Product quantum yields for reaction 11 have been determined as a function of wavelength (Figure 1). In order to interpret the results recall the conclusions of our spectroscopic and theoretical study¹⁵ of **2**. The 467-nm (ϵ 2650) band of **2** results from the $31 a' \rightarrow 32 a'$ FeN_4 localized $\pi \rightarrow \pi^*$ transition. From the orbital compositions of the $X\alpha$ calculation (Figure 2), it is evident that this transition has little

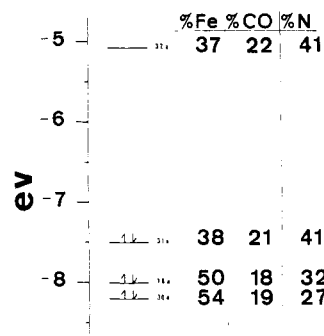


Figure 2. Frontier orbitals and their % atomic character from the $X\alpha$ calculation of $\text{Fe}(\text{CO})_3(\text{N}_4\text{H}_2)$.

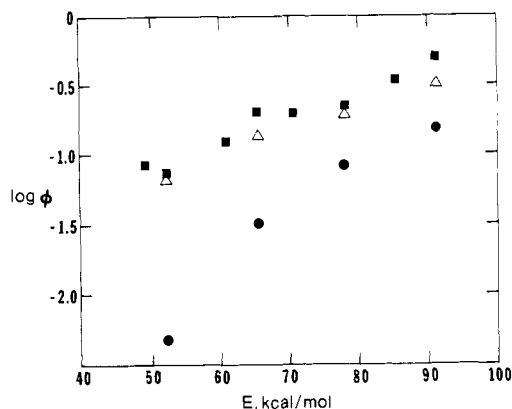


Figure 3. Plot of the log of the substitution quantum yields versus excitation energy for $\text{Fe}(\text{CO})_3(\text{N}_4\text{Me}_2)$ (\blacksquare), $\text{Fe}(\text{CO})_2(\text{PPh}_3)(\text{N}_4\text{Me}_2)$ (\bullet), and $\text{Fe}(\text{CO})_3(\text{DAB})$ (Δ).

“charge-transfer” character. The 342-nm (ϵ 3890) band arises from the nearly degenerate $18 a'' \rightarrow 32 a'$ and $30 a' \rightarrow 32 a'$ electronic transitions which exhibit slight $\text{Fe} \rightarrow \text{N}_4\text{Me}_2$ charge-transfer character. As experimental evidence for the FeN_4 localized nature of the transition, we noted¹⁵ that $\text{Fe}(\text{P}(\text{OMe})_3)_3(\text{N}_4\text{Me}_2)$ displays an absorption spectrum similar to **2**. Considering the nature of the lowest electronic transitions, we were surprised to find the high Φ 's for CO loss and the lack of correlation with the absorption spectrum. One trivial explanation for the $\Phi(\lambda)$ dependence would attribute the photochemistry to partial direct excitation of the underlying tail of an absorption band from the UV spectral regime. This scenario can be eliminated on the grounds that it requires the Φ near 400 nm (where the low-energy bands minimize) to be at least a factor of 3 greater than that observed.

Quantum yield-wavelength effects are not uncommon for transition-metal complexes, and such variations usually have been ascribed to more than one photoactive excited state.¹⁻⁷ Alternate chemical modes of reaction may also lead to quantum yield-wavelength effects. For example, $\text{Fe}(\text{CO})_3(\eta^2\text{-diene})$ intermediates may be responsible for the wavelength dependence observed for $\text{Fe}(\text{CO})_3(\eta^4\text{-diene})$ photosubstitution reactions.³⁰ No alternate chemical modes of reaction have been observed in the iron tetraazadiene complex.

A photoactive excited state model does not appear to be appropriate for rationalizing the photoreactivity of **2**, since there is little reason to expect FeN_4 localized excited states would preferentially labilize CO. Furthermore, the detailed $\Phi(\lambda)$ plot of Figure 3 does not evidence discontinuous behavior associated with a “state crossing” phenomenon.² There is a continuous increase in Φ with excitation energy that argues against the concept of some specific state at higher energy with a large Φ for dissociation.

Deuteration and Quenching Experiments. Next consider possible variations in other nonradiative decay rates. If the primary mode of physical deactivation was to the ground state, then the rate of decay might decrease as the energy gap increased³¹ and lead to

Table II. Deuteration Effect on the Quantum Yield for CO Photosubstitution by PPh_3 in 2^a

λ_{irr} , nm	$\Phi_{\text{H}}^b \pm 15\%$	$\Phi_{\text{D}}^c \pm 15\%$
313	0.44	0.44
436	0.25	0.27
546	0.075	0.076
578	0.083	0.090

^a All photoreactions at 25 °C in benzene solutions. ^b Quantum yield for 8.52×10^{-2} M 2 + 8.53×10^{-2} M PPh_3 except at 578 nm (3.06×10^{-2} M Fe + 0.300 M PPh_3). ^c Quantum yield for 8.69×10^{-3} M $\text{Fe}(\text{CO})_2(\text{N}_3(\text{CD}_3)_2)$ + 8.72×10^{-2} M PPh_3 except at 578 nm (3.68×10^{-2} M Fe + 0.401 M PPh_3).

an increase in the reaction quantum yield. A number of studies have shown that deuteration of a compound may affect the rate of nonradiative decay³² in metal complexes. Quantum yields for perdueterio and perprotio 2 (listed in Table II) are identical within experimental error. The absence of a deuteration effect on the quantum yield tends to rule out the weak coupling model³¹ and its characteristic energy gap dependence. The deuteration effect contrasts with that observed in Ru(II) coordination complexes³² where a weak coupling description seems more appropriate. Although there is no positive evidence regarding the effect of increasing excitation energy on physical deactivation, the rate probably will not decrease. Theories of nonradiative decay³³ generally predict an increase in the rate of physical deactivation at higher energies (except in the weak coupling limit³¹) because of the concomitant increase in the density of vibronic states.³⁴

Attempts to quench reaction 11 with ferrocene ($E_T = 41$ kcal/mol)³⁵ (an efficient quencher of triplet excited-state organic compounds) have been unsuccessful. Even with 0.42 M ferrocene in benzene the quantum yield at 546 nm was 0.075, identical with the unquenched quantum yield measured in a parallel run. Similarly, 0.32 M ferrocene gave a quantum yield at 366 nm of 0.22, also identical with the unquenched quantum yield. The triplet energy of ferrocene could be too high to quench excited 2 although ferrocene will quench donors with triplet energies less than 41 kcal/mol quite efficiently.³⁵ Furthermore, energetic considerations (vide infra) would not permit an excited state with energy much below 45 kcal/mol to break an Fe–CO bond. Quenching experiments with perylene (0.003 M, $E_T = 36$ kcal/mol)³⁶ were equally unsuccessful. These results are compatible with a very short excited state lifetime, although one other possible explanation is that the electronically excited iron complex reacts from a "singlet" state with little "triplet" character. The latter alternative seems unlikely due to the relaxation of spin selection rules in transition-metal complexes.

The Strong Coupling Model. Evidence for fast photodissociation from excited 2 can be found in the quantum yield vs. wavelength behavior. Conversion from upper excited states to the lowest vibronic excited-state frequently occurs rapidly.³⁷ In this case one finds a flat Φ vs. λ profile. The $\Phi(\lambda)$ behavior in 2 suggests that reaction from upper vibronic levels of several excited states competes with internal conversion. Recent reports have also indicated that photochemical reactions can proceed on a picosecond time scale and in competition with vibrational relaxation.^{28,38–40} In the case of a Cr(III) complex, the quantum yield–wavelength dependence across the low-energy side of the first quartet absorption band³⁸ suggested this type of behavior. In the light of these results, our quantum yield–wavelength dependence study merits further consideration.

(34) Jortner, J.; Rice, S. A.; Hochstrasser, R. M. *Adv. Photochem.* **1969**, *7*, 149–310.

(35) Herkstroeter, W. G. *J. Am. Chem. Soc.* **1975**, *97*, 4161–4167. Far-milo, A.; Wilkinson, F. *Chem. Phys. Lett.* **1975**, *34*, 575–580.

(36) Engle, P. S.; Monroe, B. M. *Adv. Photochem.* **1970**, *8*, 245–313.

(37) Kasha, M. *Chem. Rev.* **1947**, *41*, 401–419. Kasha, M. *Discuss. Faraday Soc.* **1950**, *No. 9*, 14–19.

(38) Sasseville, R.; Langford, C. H. *J. Am. Chem. Soc.* **1979**, *101*, 5834–5836.

(39) Spears, K. G.; Hoffland, L. *J. Chem. Phys.* **1977**, *66*, 1755–1756.

(40) Morgante, C. G.; Struve, W. S. *Chem. Phys. Lett.* **1980**, *69*, 59–60. Freedman, A.; Bersohn, R. *J. Am. Chem. Soc.* **1978**, *100*, 4116–4118.

Table III. Temperature Effect on the Quantum Yield for CO Photosubstitution by PPh_3 in 2 and Calculated Apparent Activation Energies^a

λ_{irr} , nm	T , K	$10^3 C_{\text{Fe}}$, M	$10^3 C_{\text{PPh}_3}$, M	Φ	E_{app}
578	308.5	32.1	321	0.079 ^b	–2.5
578	308.2	32.2	327	0.063 ^c	
578	307.7	30.6	300	0.078 ^c	
578	298.0	32.2	327	0.083	
578	298.0	32.2	327	0.082	
578	290.1	30.6	300	0.087	+2.2
578	282.5	32.1	321	0.111	
546	308.0	9.92	104	0.097	
546	308.0	9.19	104	0.084	
546	308.0	9.19	104	0.094	
546	298.0	9.90	104	0.076	
546	298.0	9.84	116	0.078	
546	298.0	5.35	110	0.070	
546	288.0	9.92	104	0.072	
546	282.2	9.19	104	0.065	
436	308.3	1.07	12.6	0.208	+1.6
436	298.0	0.55	3.44	0.194	
436	282.7	1.07	12.6	0.164	

^a Calculated from Arrhenius activation energy plots, in kcal/mol, estimated error ± 1 kcal/mol. ^b Includes a 12% correction for thermal reaction. ^c Includes a 20% correction for thermal reaction.

Most discussions of the photochemistry of Werner complexes and organo-transition-metal compounds have focused on the properties of specific types of excited states, and we believe that the strong coupling limit has not been adequately recognized. The latter model might be simply described as conversion of excited state energy into vibrational motions within the molecule. This vibrational excitation leads to dissociation *before* vibrational deactivation within a specific excited state can take place. Crudely put, the molecule briefly rattles around until either physical deactivation to the ground state occurs or it finds a reaction channel. One should also recognize that the excited state will not achieve thermal equilibrium³¹ on the time scale of the reaction. In this limit the strong coupling between the initially prepared vibronic state and the dissociation continuum acts to deemphasize the nature of specific electronic states; however, the electronic excitation can influence which vibrational modes initially receive the energy. We introduce the premise that *only a relatively constant fraction of the excitation energy is available for the Fe–CO dissociative process*. A quasi-statistical³³ partitioning of energy would be favored by (1) dense manifolds of vibronic levels, (2) lack of symmetry selection rules on the nonradiative decay pathways, and (3) delocalized excited electronic states that do not couple strongly with any single vibrational mode; we qualify condition 3 by noting that even localized excitations can lead to "statistical" behavior.³⁴ The word "statistical" is not used in a thermal sense, because the partitioning of the excitation energy depends on the specifics of intramolecular vibronic coupling.

Simple experimental manifestations that might be expected include the following: (1) quantum yields for photodissociative pathways that depend on the amount by which the excitation energy exceeds the thermodynamic threshold; (2) multiple reaction pathways that become increasingly available at higher excitation energies; (3) because the energy flow relies on the vibrational modes that initially receive the energy and how they couple with other modes, there should be a structure sensitivity to the reaction quantum yields; (4) the exact antibonding nature of the excited state becomes irrelevant. In practice, the descriptions of real chemical systems may lie somewhere between the weak and strong coupling models.

Recent experiments place the $\text{Fe}(\text{CO})_4$ –CO bond dissociation energy at 55 ± 12 kcal/mol.⁴¹ In solution the enthalpy of ac-

(41) Engelking, P. C.; Lineberger, W. C. *J. Am. Chem. Soc.* **1979**, *101*, 5569–5573.

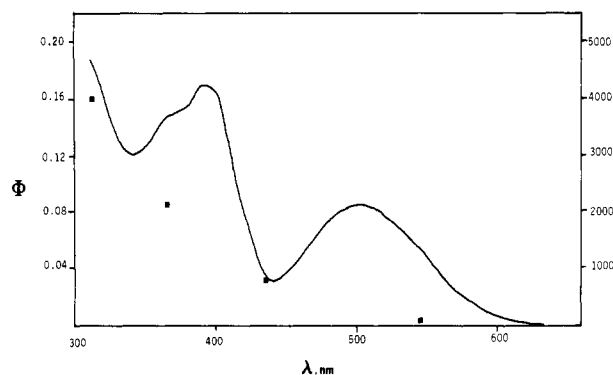


Figure 4. Quantum yields for the photosubstitution reaction $\text{Fe}(\text{CO})_2(\text{PPh}_3)_2(\text{N}_4\text{Me}_2) + \text{PPh}_3 \rightarrow \text{Fe}(\text{CO})(\text{PPh}_3)_2(\text{N}_4\text{Me}_2) + \text{CO}$, plotted vs. wavelength, along with the absorption spectrum of the reactant.

tivation⁴² of 43 kcal/mol for Fe–CO dissociative reactions provides a reasonable estimate of the bond strength. The wavelength 578 nm corresponds to a photon energy of 49.5 kcal/mol, and the potential for a thermodynamic bond dissociation energy barrier does exist in iron carbonyl complexes, especially if one considers that not all of the absorbed energy will be channeled into the bond-breaking process. We have previously noted¹⁵ the similarity between the average C–O stretching frequencies in **2** and $\text{Fe}(\text{CO})_5$. Therefore, one expects comparable metal–carbonyl bond energies in the two complexes.

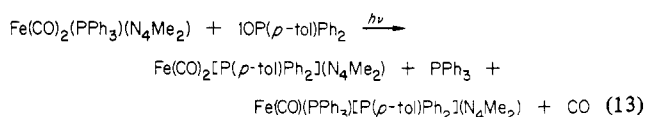
An immediate question is whether the excited state can acquire thermal energy from solvent to aid in the dissociation. Although this would not be possible in the strong coupling limit, it does have precedent in the photochemistry of Werner complexes in the concept of the excited state processes.⁴³ Quantum yield data and Arrhenius activation energies (E_{app}) are summarized for several wavelengths in Table III. The near-zero values for E_{app} clearly indicate that the excited state can not acquire appreciable thermal energy from its environment to aid in bond-breaking processes. At first, the nearly identical 578- and 546-nm quantum yields seem inconsistent with the threshold arguments; however, the red tail (525–600 nm) of the electronic absorption band disappears at low temperature¹⁵ because it arises from hot bands. One achieves nearly the same net excited-state energy in hot-band excitation, the irradiation energy difference being made up by the selective excitation of a hot fraction of ground-state molecules. Since the quantum yield is normalized according to the ϵ at each λ , it should not change greatly as one irradiates different hot-band spectral regions.

As further evidence supporting the strong coupling model, we note (Figure 3) an approximately linear correlation between $\log \Phi$ and the energy of irradiation. Although the plot should level off when $\Phi \approx 1$, we could not extend measurements further into the UV due to interfering solvent and ligand absorptions. This pseudo linear-free-energy relationship illustrates the importance of the net excitation energy, rather than the nature of specific excited states. To test the generality of these conclusions, we examined related systems.

Photosubstitution in Structurally Related Complexes. Monophosphine iron tetraazadiene complexes have electronic spectra quite analogous in appearance to the parent tricarbonyl complex and exhibit low-energy bands slightly red-shifted from corresponding features in the tricarbonyl complex.¹⁵ Reaction 9 ($\text{L} = \text{PPh}_3$) proceeds cleanly to the bis(phosphine) product without further substitution. Quantum yields for this process and the spectrum of the parent complex (Figure 4) again evidence little correlation between the two properties; however, the Φ 's rise exponentially with increasing energy, just as for the first substitution (see plots of Figure 3). Compared with the first ligand

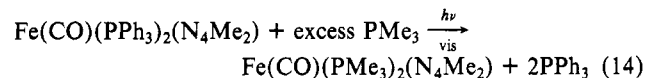
substitution process, the Φ 's for loss of the second CO diminish considerably (at similar wavelengths) despite the spectral similarities. Reduced efficiency for more extensive CO photosubstitution by phosphorus ligands appears to be a common phenomenon in organometallic photochemistry, although little quantum yield data has been reported.^{6,9,44} Replacement of CO with the weaker π -acceptor ligand PPh_3 is usually thought to result in stronger bonds between the metal and the remaining CO ligands. Bond length data for $\text{Mn}(\text{NO})(\text{CO})_4$ and $\text{Mn}(\text{NO})(\text{CO})_3(\text{PPh}_3)$ support this explanation.⁴⁵ In the framework of the strong coupling model, this should lead to reduced quantum efficiencies owing to the lesser amount by which the excitation energy exceeds the thermodynamic threshold. Furthermore, the additional vibrational modes of PPh_3 (and the fact that there is one less CO) diminish the probability of channeling the excitation energy into Fe–CO bond breaking.

The quantum yield also shows negligible dependence on the PPh_3 concentration (Tables II of the supplementary material) or when $\text{L} = \text{PMe}_3$, again suggesting a dissociative mechanism; however, the possibility exists for loss of either CO or PPh_3 . We considered the alternative explanation that the relatively small quantum yields as well as the wavelength behavior might arise due to competing loss of PPh_3 . Capture of the putative intermediate by PPh_3 then regenerates the reactant. Reaction 13 was followed by ³¹P NMR



to test this point. Irradiation at wavelengths longer than 400 nm gave >90% of the bis(phosphine) product resulting from CO loss. The same result is obtained by irradiation at ~ 365 nm. In the control experiment we proved that discrimination between the two phosphine ligands by the coordinately unsaturated intermediate does not complicate the interpretation.

Photochemical loss of the third CO ligand proceeds even less efficiently and has not been studied in detail; however, $\text{Fe}(\text{CO})(\text{PPh}_3)_2(\text{N}_4\text{Me}_2)$ is nonetheless photoactive as can be seen from reaction 14.



As a test of the transferability of the photochemical reactivity to systems with related geometrical structures, but different electronic properties, we investigated the diazabutadiene (DAB) complex²¹ **1**. The IR data suggests that the DAB ligand is not as good a π acceptor as the tetraazadiene ligand (average CO stretching frequencies $\bar{\nu} = 1983 \text{ cm}^{-1}$ for DAB vs. weighted $\bar{\nu} = 2019 \text{ cm}^{-1}$ for tetraazadiene complex). Consequently, the nature of the iron–metallocycle π bonding must be altered. Iron DAB complexes similar to **1** exhibit an intense electronic absorption band in the vicinity of 500 nm.^{14,46} This band has been assigned as metal to DAB charge transfer by analogy to the much studied $\text{Mo}(\text{CO})_4(\text{DAB})$ complexes.⁴⁶ Additional evidence cited for this assignment was the lack of CO substitution observed upon irradiation into the low-energy absorption. We find the position of the low energy electronic transition in **1** to be essentially solvent insensitive ($\lambda_{\text{max}}(\text{solvent})$ 507 nm (CH_3OH), 508 (CH_2Cl_2), 508 (benzene)) in contrast to the great solvent sensitivity of the $\text{Mo}(\text{CO})_4(\text{DAB})$ bands.⁴⁷ Furthermore, complex **1** is not photoinert when the low-energy band is excited. These results do not conclusively argue against a charge-transfer assignment but do

(42) Siefert, E. E.; Angelici, R. J. *J. Organomet. Chem.* **1967**, *8*, 374–376.

(43) Martin, J. E.; Adamson, A. W. *Theor. Chim. Acta* **1971**, *20*, 119–134. Chen, S.-N.; Porter, G. B. *Chem. Phys. Lett.* **1970**, *6*, 41–42. Adamson, A. W. *Pure Appl. Chem.* **1979**, *51*, 313–329.

(44) Alway, D. G.; Barnett, K. W. *Inorg. Chem.* **1980**, *19*, 1533–1543.

(45) Frenz, B. A.; Enemark, J. H.; Ibers, J. A. *Inorg. Chem.* **1969**, *8*, 1288–1293.

(46) tom Dieck, H.; Orloff, A. *Angew. Chem., Int. Ed. Engl.* **1975**, *14*, 251–252; *Angew. Chem.* **1975**, *87*, 246–247.

(47) Bock, H.; tom Dieck, H. *Chem. Ber.* **1967**, *100*, 228–246.

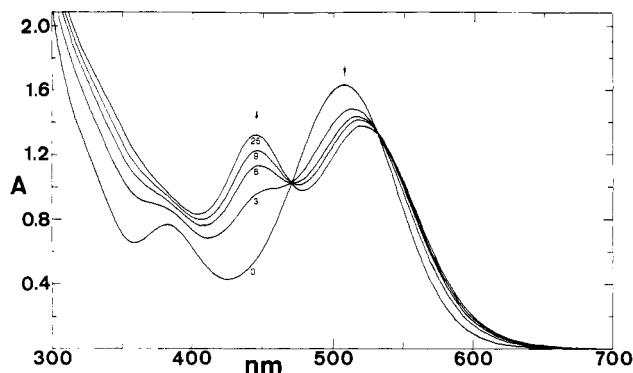


Figure 5. Electronic absorption spectral changes during photolysis of a 1.9×10^{-3} M benzene solution of $\text{Fe}(\text{CO})_3(\text{DAB})$, containing a fivefold excess of PPh_3 . Irradiation times (min) are shown for a 200-W HgXe arc lamp source with a Corning 0-52 filter ($\lambda > 340$ nm).

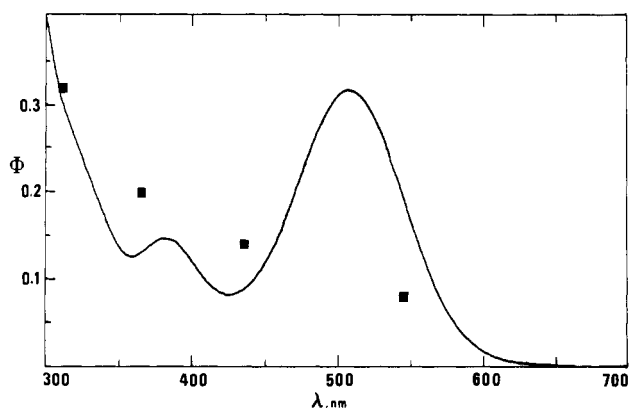
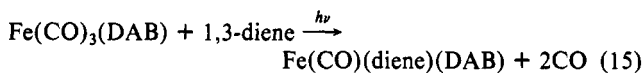


Figure 6. Quantum yields for the photosubstitution reaction $\text{Fe}(\text{CO})_3\text{-(DAB)} + \text{PPh}_3 \rightarrow \text{Fe}(\text{CO})_2(\text{PPh}_3)(\text{DAB}) + \text{CO}$, plotted vs. wavelength, along with the absorption spectrum of the reactant.

weaken the purported analogy between the iron and molybdenum DAB complexes.

Photolysis of solutions of the $\text{Fe}(\text{CO})_3(\text{DAB})$ complex in the presence of excess PPh_3 leads to clean substitution with no secondary photolysis as evidenced by Figure 5. Reasons for lack of formation of a bis(phosphine) complex may be steric or thermodynamic in nature. With the smaller, better π -acceptor ligand $\text{P}(\text{OMe})_3$, the disubstituted product is generated.

Quantum yields for CO loss with entering PPh_3 are plotted vs. wavelength in Figure 6. The efficiency is quite higher, even for irradiation into the low-energy band where CO substitution was reported to be inefficient.⁴⁶ The previous study referred to reaction 15 and the lack of reactivity may result from a low photosub-



stitution efficiency of CO in a dicarbonyl-(η^2 -diene) intermediate. The quantum yields are very similar to those for the tetraazadiene complex, both in magnitude and in their wavelength dependence (see Figure 3). Perhaps this illustrates a connection between quantum yields and geometry, since both complexes possess common coordination structures. As before, the quantum yields correlate better with the net excitation energy than with the character of the excited state reached.

Summary

Photochemical reaction of **2** and related complexes proceed via dissociative loss of CO, while thermal reactions transpire via associative pathways. As predicted by Strohmeier,⁴⁸ the preparative applications of photochemistry are especially useful in this instance. Photosubstitution of CO occurs with high quantum efficiencies in the tetraazadiene and diazabutadiene complexes even though the lowest energy excited states are metalocycle localized. The magnitude of the photosubstitution quantum yield increases exponentially with excitation energy. A strong coupling description rationalizes the photochemical behavior of these complexes. In this model the amount by which the excitation energy exceeds the thermodynamic threshold for dissociation acquires considerable importance. Limited observations raise the possibility that there may be some connection between the coordination environment about the iron atom and the quantum efficiencies for ligand substitution. The possible influence of molecular structure on photochemical reactions was suggested by Hammond,⁴⁹ but there have been few such studies of transition-metal complexes. Fragmentation of the tetraazadiene ligand (N_2 extrusion) has not been observed with the iron carbonyl complexes. Contrast this behavior with isoelectronic⁵⁰ $\text{Co}(\eta^5\text{-C}_5\text{H}_5)(\text{N}_4\text{R}_2)$ compounds, which do not possess a readily dissociable ligand and cleanly lose N_2 when metalocycle localized transitions are excited.⁵¹

Acknowledgment. We thank the National Science Foundation (Grant CHE78-01615) for support of this research.

Supplementary Material Available: Experimental details describing the reaction between **2** and diphos, photolysis of **2** to produce **3**, photolysis of **2** with added $\text{Fe}(\text{CO})_5$, photolysis of $\text{Fe}(\text{CO})_2(\text{PPh}_3)(\text{N}_4\text{Me}_2)$ with added $\text{P}(\text{P-tol})\text{Ph}_2$, photolysis of $\text{Fe}(\text{CO})(\text{PPh}_3)_2(\text{N}_4\text{Me}_2)$ with added PMe_3 , the photochemical synthesis of $\text{Fe}(\text{CO})(\text{dmpe})(\text{N}_4\text{Me}_2)$, and photolysis of $\text{Fe}(\text{CO})_3(\text{DAB})$ with added PPh_3 or $\text{P}(\text{OMe})_3$, a table of extinction coefficients used to calculate quantum yields, and a table of quantum yields for the photosubstitution of CO in $\text{Fe}(\text{CO})_2\text{-(PR}_3)(\text{N}_4\text{Me}_2)$ (6 pages). Ordering information is given on any current masthead page.

(48) Strohmeier, W. *Angew. Chem., Int. Ed. Engl.* **1964**, *3*, 730-737.

(49) Hammond, G. S. *Adv. Photochem.* **1969**, *7*, 373-391.

(50) Gross, M. E.; Trogler, W. C.; Ibers, J. A. *J. Am. Chem. Soc.* **1981**, *103*, 192-193.

(51) Gross, M. E.; Trogler, W. C. *J. Organomet. Chem.* **1981**, *209*, 407-414.